Proc. Natl. Acad. Sci. USA
Vol. 79, pp. 574–578, January 1982
Immunology

Polymerization of the ninth component of complement (C9): Formation of poly(C9) with a tubular ultrastructure resembling the membrane attack complex of complement

(protein–protein interactions/protein–phospholipid interactions/protein polymerization/transmembrane channels)

ECKHARD R. PODACK AND JÜRG TSCHOPP

Department of Molecular Immunology, Research Institute of Scripps Clinic, La Jolla, California 92037

Communicated by Hans J. Müller-Eberhard, September 1, 1981

ABSTRACT **The ninth component of complement (C9) has a marked propensity to polymerize. C9 polymers [poly(C9)] formed spontaneously in Veronal-buffered saline upon incubation of purified C9 for 64 hr at 37°C or within 2 hr at 46–56°C. Poly(C9) formed at 37°C was visualized by electron microscopy as a tubular structure with an internal diameter of 110 Å and a length of 160 Å. Its ultrastructure suggested a dodecameric composition and resembled that of the membrane attack complex of complement. The wider end of the tubular structure was formed by an ≈30-Å-thick torus with inner and outer diameters of 110 Å and 220 Å, respectively. Because the dimensions of C9 within poly(C9) were 160 × 55 Å (maximal) and 20 Å (minimal) and because monomeric C9 has dimensions of approximately 80 × 55 Å, it is proposed that monomeric C9 unfolds during polymerization into tubules. Polymerization also occurred upon treatment of C9 for 1 hr at 37°C with 0.6 M guanidine·HCl, 0.1 M octyl glucoside, or 1.5% sodium deoxycholate. Guanidine·HCl-induced C9 polymers consisted of elongated highly curved strands 55–80 Å wide, suggesting that these polymers were formed by globular C9 that had not unfolded.**

The ninth component (C9) is the last protein that binds to the assembling membrane attack complex (MAC) of complement, completing the sequence of events that leads to the destruction of target membranes. Although lysis of erythrocytes occurs even without C9 (1), its presence increases the rate of hemolysis (2).

C9-mediated hemolysis is a relatively slow (3) and temperature sensitive reaction (2, 4, 5) and has therefore been attributed to an enzymatic action of C9 (5). Multiple C9 molecules bind to C5b–8 in forming the MAC (6–8), and it has been postulated that the C9 to C8 ratio determines the size of transmembrane channels formed by C5b–9 (9, 10). Studies with photoactivatable membrane-restricted probes suggested that C9 subunits of the MAC penetrate the hydrocarbon core of the lipid bilayer more deeply than does any other subunit of the MAC (11, 12). C9 within the membrane-bound MAC is also accessible from the aqueous phase, suggesting that the MAC-associated C9 extends from the hydrophilic phase into the hydrocarbon phase of the membrane (11).

Ultrastructural studies demonstrated that formation of the ring-like membrane lesion caused by complement is entirely dependent on C9 (13, 14) and that C9 mediates the fusion of two C5b–8 complexes to the characteristic ring structure of the dimeric MAC (14). Both C5b–9 dimerization and C9-mediated hemolysis (2) are temperature-sensitive reactions (15), suggesting an important role of C9 for dimer formation in the cytolytic reaction. The dimeric nature of the MAC was supported by molecular weight studies (16) and by molecular hybridization experiments (17). Subsequent studies (unpublished) indicated a tendency of the MAC to form MAC oligomers (18). In contrast, other groups suggested a monomeric C5b–9 composition of the MAC (19, 20).

The present communication demonstrates the propensity of purified C9 to form polymers [termed poly(C9)] and presents evidence indicating that C9 polymerization within the MAC represents the molecular mechanism of C9 action.

MATERIALS AND METHODS

C5 and C9 were purified from human serum according to Hammer *et al.* (21). As a final step for C5 purification, affinity chromatography on concanavalin A-Sepharose 4B was used. The final step for C9 purification was hydroxylapatite chromatography as described by Biesecker and Müller-Eberhard (22). C6, C7, and C8 were purified from human serum as described (23, 24).

Hemolytic assays for C5, C6, C7, C8, and C9 were performed by using the respective depleted sera and sheep EA as described previously for C6 and C7 (23). Samples containing guanidine·HCl (Gdn·HCl) were diluted at least 1:100 prior to the assay. Diluted Gdn·HCl did not interfere with the hemolytic assay.

For polymerization of C9, purified C9 was diluted to 0.4 mg/ml in Veronal- (barbital, 3.3 mM, pH 7.4) buffered 0.15 M saline containing 0.15 mM $CaCl_2$ and 0.5 mM $MgCl_2$ (VB). Spontaneous polymerization was achieved by incubating this solution for 64 hr at 37°C in the presence or absence of 2 mM phenylmethylsulfonyl fluoride and soybean trypsin inhibitor at 50 μg/ml. Heat-induced polymerization followed incubation of C9 in Veronal-buffered saline for 30 min to 2 hr at 46–56°C. Chemically induced polymerization was initiated by adding to C9 Gdn·HCl, octyl glucoside, or sodium deoxycholate to a final concentration of 1 M, 0.1 M, or 1.5%, respectively, and incubating the mixture for 1 hr at 37°C. Deoxycholate treatment was carried out at pH 8.1 in 20 mM Tris acetate/0.09 M NaCl/0.2 mM EDTA/0.02% sodium azide.

C5, C6, C7, and C8 were incubated with 1 M Gdn·HCl under identical conditions as described for C9. C7 was also incubated at 37°C for 64 hr or at 56°C for 1 hr as above.

Ultracentrifugation was carried out in the model E analytical ultracentrifuge (Beckman) at various centrifugal forces. The rate of sedimentation was determined with an optical scanner at 280 nm. The absorbance of a solution containing C9 at 1 mg/ml was

The publication costs of this article were defrayed in part by page charge payment. This article must therefore be hereby marked "*advertisement*" in accordance with 18 U. S. C. §1734 solely to indicate this fact.

Abbreviations: C9, the ninth component of complement; Ans, 1-anilinonaphthalene-8-sulfonic acid; VB, 3.3 mM Veronal-buffered 0.15 M saline (pH 7.4)/0.15 mM $CaCl_2$/0.5 mM $MgCl_2$; MAC, membrane attack complex of complement (C5b–9 dimer); Gdn·HCl, guanidine hydrochloride.

0.96 and that of C8 at 1 mg/ml was 1.6 as determined by recording the absorption spectrum in a Cary 219 spectrophotometer (Varian) and measuring the protein content by amino acid analysis. Light scattering was determined at 385 nm at a 90° angle to the incident light in an Aminco Bowman spectrofluorometer (American Instrument). 1-Anilinonaphthalene-8-sulfonic acid (Ans) fluorescence was determined in the same instrument at 50 μM final concentration. The uncorrected spectra are shown. A Hitachi model 12A (Tokyo) was used for electron microscopy after samples were negatively stained with 2% uranyl formate, 2% uranyl acetate, or 1.5% sodium phosphotungstate (pH 7.2) by the pleated sheet technique (25).

RESULTS

Formation of Tubular C9 Polymers. Purified C9 spontaneously formed high molecular weight homopolymers in VB upon incubation at 37°C for 64 hr or for 1–2 hr at 46–56°C. Polymerization occurred in the absence or presence of 10 mM EDTA. Heat-induced poly(C9) sedimented at more than 40 S.

Fig. 1 depicts the ultrastructural appearance of spontaneously polymerized C9. The field viewed at low magnification (panels 1 and 2) showed that C9 upon incubation at 37°C for 64 hr formed hollow tubular complexes, most of which aggregated. Both top views (rings, black arrows) and side views (rectangles, black arrowheads) are seen in Fig. 1, panels 1 and 2. The poly(C9) tubules had an internal diameter of approximately 100 Å and a length of 160 Å. One end of the tubule terminated in a 30 Å-thick torus (white arrowheads) with an inner and outer diameter of 100 Å and 200 Å, respectively. The "C9 heads" (white arrowheads) formed these toruses, whereas "C9 tails" (white arrows) at the opposite end of the tubular complex aggregated individual complexes and, therefore, may constitute hydrophobic domains. The length of this presumed hydrophobic domain is estimated to be 40 Å by measuring the overlapping areas in staggered poly(C9) aggregates (Fig. 1, parallel black arrows, panels 2, 3, 9, and 10). Poly(C9) tubules probably are formed by 12 C9 molecules, judging from the subunit structure seen in many cases in top views (Fig. 1 asterisk, panels 3, 5, 6, and 7). Measurements taken from electron micrographs of

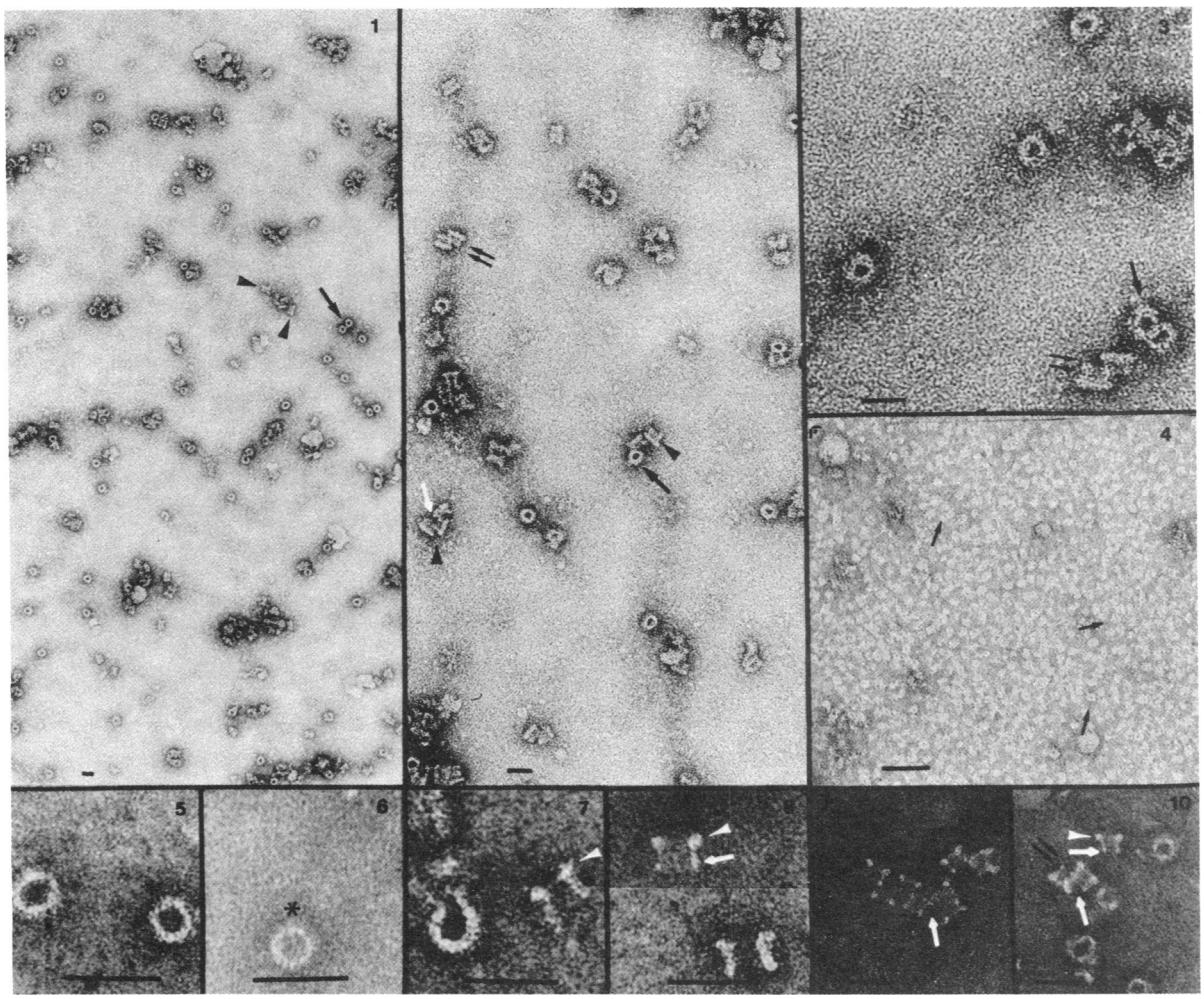

FIG. 1. Ultrastructure of monomeric C9 (panel 4) and of poly(C9) formed in VB (all other panels) at 37°C, 64 hr. Panels 1 and 2 are low-magnification field views. Panels 3–10 are high-magnification views of smaller areas. The scale bars represent 400 Å. Note the globular structure of monomeric C9 (panel 4) and the presence of stain inside the molecule (black arrows). Poly(C9) (panels 1–3 and 5–10) appears as ring structure (top view, black arrows) or as rectangular structures (side views, black arrowheads). In side views the torus (C9 heads, white arrowheads, panels 7, 8, and 10), the hydrophobic segment (C9 tails, white arrows, panels 2 and 8–10) and an intervening segment may be distinguished. Note the overlapping area (parallel black arrows, panels 2, 3, 9, and 10) presumably corresponding to the length of the hydrophobic segment. A dodecameric composition of poly(C9) is inferred from the subunit structure of several top views indicated with an asterisk (panels 3, 5, 6, and 7). C9 in panels 1, 2, and 3 was stained with uranyl acetate; in panels 4, 5, 7, and 8 lower it was stained with uranyl formate; in panels 6, 8 upper, 9, and 10 it was stained with sodium phosphotungstate.

poly(C9) indicated the length of individual C9 molecules forming the polymeric complex to be 160 Å, their width 40 Å, and their thickness 20 Å (Fig. 1, panels 7 and 8). Three domains were distinguished: C9 heads (≈30 Å of the length) forming the torus in poly(C9), an intervening sequence of about 90 Å (hinge ?), and C9 tails (40 Å) constituting the hydrophobic domain. Distal to the heads C9 is 15–20 Å thick, as indicated by the thickness of the tubular wall.

In contrast to poly(C9), monomeric C9 had a globular appearance (Fig. 1, panel 4) with approximate dimensions of 55 × 80 Å; however, substructure was not clearly visible even though negative stain usually penetrated the inside of the globular C9 monomer (Fig. 1, arrows, panel 4).

Comparing the ultrastructures of C9 in monomeric and polymeric forms, we suggest that polymerization involves unfolding of the ≈80 Å-long monomer to a 160 Å-long molecule. Simultaneously, hydrophobic domains may be exposed in poly(C9) that were hidden in monomeric C9. C9 polymerization was accompanied by a more than 2-fold increase of Ans fluorescence, suggesting binding of the fluorescent probe to newly acquired hydrophobic sites on poly(C9). The initial rates of Ans binding as a function of C9 polymerization at various temperatures are shown in Fig. 2. No polymerization occurred below 40°C within 2 hr. At 56°C the reaction was complete within 5 min. For comparison the temperature dependence of C9-mediated hemolysis and of Gdn·HCl-induced C9 polymerization (see below) is also shown.

Polymerization of C9 is accompanied by the loss of hemolytic activity. In Table 1 the loss of activity of C9 incubated for 2 hr at various temperatures and the increase of Ans fluorescence are compared with the decrease of C9 monomer (4.5S) as measured in the analytical ultracentrifuge. Both loss of activity and Ans binding correlate with C9 polymerization. Electron microscopic examination of these C9 polymers showed the formation of tubular structures at 40°C and 46°C, whereas at higher temperatures elongated C9 polymers described below predominated.

Formation of Elongated C9 Polymers. Polymerization also proceeded upon incubation of C9 for 1 hr at 37°C with 0.6 or 1 M Gdn·HCl (Fig. 3), 0.1 M octyl glucoside, or 1.5% sodium deoxycholate. Table 2 summarizes the observed sedimentation rates of C9 polymerized by these means as determined in the analytical ultracentrifuge. Poly(C9) formed by Gdn·HCl, detergents, or heat was polydisperse, indicating various molecular sizes.

Poly(C9) generated by treatment with Gdn·HCl (Fig. 3) formed extended, curved strands of various lengths and an average width of 50–80 Å. Occasionally C9 rings with inner and outer diameters of 100 Å and 200 Å, respectively, were seen; however, no polymers with 160-Å width were detectable. This finding suggested polymerization of globular C9 without attendant unfolding.

Specificity of Tubular Polymerization for C9. In control experiments, the other terminal complement proteins C5, C6, C7, and C8 were subjected to the same treatments that polymerized C9; Table 3 summarizes the results. Notably, C7 responded to Gdn·HCl treatment with a polymerization reaction similar to that of C9; however, no tubular or ring structures were detected in the electron microscope. In addition, C7 was in-

Table 1. Correlation of C9 polymerization, loss of hemolytic activity, and Ans binding

Temperature, °C	Loss of hemolytic activity, % of total	Increase of Ans fluorescence, % of total	Decrease of monomeric C9, % of total
4	0	0	0
40	7.7	9.6	11
46	17	25	33
52	92	76	86
56	98	94	94

C9 was incubated at 0.4 mg/ml in 10 mM Tris·HCl- (pH 7.4) buffered 0.15 M NaCl for 2 hr at the indicated temperatures. Samples were then analyzed for hemolytic activity, Ans fluorescence, and sedimentation in the analytical ultracentrifuge.

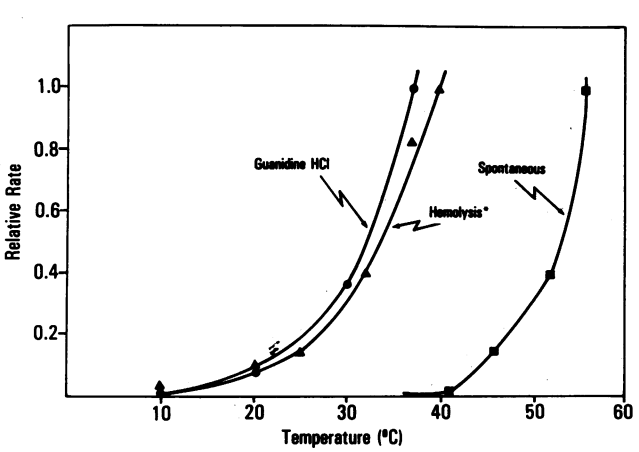

FIG. 2. Comparison of initial rates of heat-induced C9 polymerization, of Gdn·HCl-induced C9 polymerization, and of C9-mediated hemolysis at various temperatures. Data for C9-mediated hemolysis are taken from Hadding and Müller-Eberhard (2). Gdn·HCl-mediated C9 polymerization was measured by the increase of light scattering, and heat-induced polymerization was followed by the increase of Ans fluorescence. The initial rates of C9 polymerization and hemolysis in the linear part of the progress curves are compared. The initial rate at the highest temperature measured was arbitrarily set to one and the rates at the lower temperatures are expressed as fraction of the maximal rate observed.

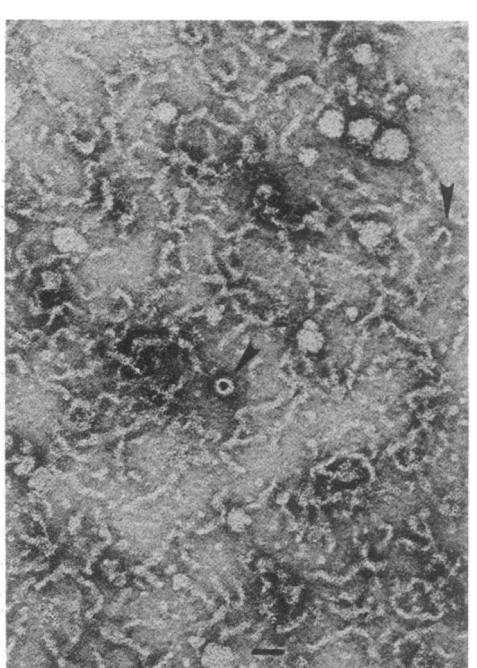

FIG. 3. Ultrastructure of Gdn·HCl-induced C9 polymers. The scale bar represents 400 Å. Highly curved structures of ≈50 Å width (black arrowheads) and linear structures of ≈80 Å width are shown. Negative stain with uranyl formate.

Table 2. Sedimentation rate of poly(C9)

Treatment			Observed sedimentation coefficient, S
Time, hr	Temp., °C	Solvent	
1	37	VB	4.5
1	37	0.3 M Gdn·HCl	4.5
1	37	0.6 M Gdn·HCl	27 (21–33)*
1	37	1 M Gdn·HCl	27 (21–33)*
1	37	4 M Gdn·HCl	3.7
1	37	0.1 M octyl glucoside	34.5 (21–48)*
1	37	1.5% deoxycholate	9 (7–11)*
0.5	56	VB	>40
64	37	VB	>40

* Observed sedimentation range.

sensitive to prolonged incubation at 37°C or to increased temperatures. Like Gdn·HCl-induced poly(C9), C7 polymers were hemolytically inactive but became reactivated and monomerized by incubation with 4 M Gdn·HCl. The anomalous increase of the sedimentation rate of C5 and C6 (Table 3) in 1 M Gdn·HCl may indicate increased but reversible self-association. Gdn·HCl (26) (Table 3) and chaotrope treatment (27) of C5 resulted in inactivation without polymerization, whereas C6 and C8 were not inactivated, or only partially so, respectively. The C8 subunits apparently dissociate upon incubation with 1 M Gdn·HCl (Table 3), then spontaneously reform intact C8 upon removal of the chaotrope, similar to the effect of sodium dodecyl sulfate on C8 (28, 29).

DISCUSSION

This publication defines the conditions for polymerization of C9 in isolated form and describes the properties of the so-formed poly(C9). Understanding the polymerization reaction of C9 allows one to interpret the cytolytic mechanism of the MAC and the ultrastructural changes accompanying C9 binding under the premise that C9 undergoes polymerization upon binding to C5b–8. In addition, the spontaneous polymerization of purified C9 provides a model reaction for the transformation of water-soluble molecules into a macromolecular, amphiphilic complex with membranolytic activity (30).

Ultrastructural analysis of monomeric native C9 and of molecules constituting the tubule that poly(C9) forms leads to the conclusion that C9 unfolds during or subsequent to its polymerization. Fig. 4 contains the dimensions of poly(C9) and of

Table 3. Sedimentation velocity and activity of terminal complement components after treatment with 1 and 4 M Gdn·HCl

	Observed sedimentation coefficient, S		Hemolytic activity,* % of control	
Protein	VB	1 M Gdn·HCl	1 M Gdn·HCl	4 M Gdn·HCl‡
C5	8.1	8.9	0	0
C6	5.5	6.3	90	95
C7	*5.3*	*22.7*†	*5*	*93*
C8	8.1	3.8	88	58
C9	*4.5*	*27*†	*0*	*100*
HSA	4.5	3.9	NA	NA

HSA, human serum albumin; NA, not applicable.
* Hemolytic activity determined after 1:100 dilution of Gdn·HCl-containing samples.
† Mean of the observed sedimentation coefficient; the range was ±6S.
‡ The 4 M Gdn·HCl was added subsequent to incubation with 1 M Gdn·HCl.

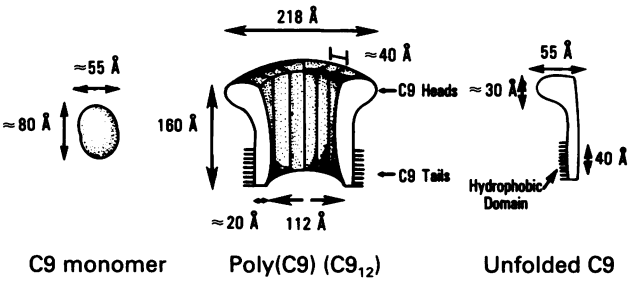

FIG. 4. Schematic representation of the dimensions of C9 in monomeric and polymeric form. The dimensions indicated are the mean values of at least 10 molecules measured. The size of unfolded C9 is deduced from the size of poly(C9) assuming a dodecameric composition.

monomeric C9. The exact ultrastructure of monomeric C9 is not certain at present because of its small size and the limited electron microscopic resolution. Monomeric C9 apparently has a globular structure whose longest dimension is ≈80 Å. In contrast, the length of C9 in its polymerized form is 160 Å. Moreover, this form exposes a hydrophobic domain of 40 Å length that is not apparent in monomeric C9. This hydrophobic site may be concealed within the protein's interior in monomeric C9.

The structure of C9 in the polymeric form can be analyzed in some detail owing to the redundancy of information. On the basis of the electron microscopic evaluation (Fig. 1) of subunit structure and size of poly(C9) one can deduce the dodecameric subunit composition, even though this value should be considered tentative until precise molecular weight measurements are available. Poly(C9) tubules have a hollow and apparently hydrophilic core of ≈100 Å diameter. Its three domains compose the torus formed by the C9 heads, the hydrophobic area constituting the membrane binding site and formed by the C9 tails, and the intervening segment connecting heads and tails. This segment may contain a hinge region allowing the transformation of globular C9 monomers into poly(C9). The 40 Å hydrophobic domain probably represents the site of attachment of photoactivatable membrane-restricted probes (11, 12), whereas the torus might be the site of radioiodination in surface labeling experiments (11).

C5b–8 may reduce the activation energy of C9 polymerization. The cytolytic reaction of C9, upon binding to cell bound C5b–8, is in fact much more rapid than spontaneous C9 polymerization (Fig. 2). Gdn·HCl-mediated C9 polymerization also is more rapid than spontaneous polymerization at 37°C. The activation energies for Gdn·HCl-mediated and spontaneous C9 polymerization are estimated to be ≈15 kcal/mol and ≈40 kcal/mol, respectively (1 kcal = 4.18 kJ). In this regard Gdn·HCl may mimic one function of C5b–8: namely, decrease the activation energy of C9 polymerization, without, however, providing a hydrophobic binding site for poly(C9).

Indirect evidence that C9 polymerizes upon reacting with C5b–8 is based on the binding of multiple C9 molecules per MAC (6, 7), on the temperature dependence of both C9 polymerization (Fig. 2) and cytolysis (2, 4, 5), on the similar ultrastructure of poly(C9) (Fig. 1) and the MAC (13, 14, 16, 17, 19, 20, 31), and on the requirement for C9 binding in formation of ultrastructural complement lesions representing the membrane-bound MAC (13, 14). The present study suggests that poly(C9) represents the structure previously ascribed to the C5b–9 complex (13, 14, 19, 20, 31). The structure of C5b–8 (14) in the membrane attack complex (16) apparently is bound adjacent to the poly(C9) tubule without contributing to the ultrastructural appearance of the membrane lesion.

Functionally, C9 may be a channel-forming molecule, the

channel being poly(C9) itself. In fact, single bilayer vesicles with isolated C9 effectively released markers in the absence of other complement proteins (30), and C9 increased the conductance of black lipid membranes (32). The precise relationship of C9 polymerization to the size of functional transmembrane channels (9, 10, 33–38) formed by the MAC is not known at present, and the question remains open whether protein channels (39) or lipid reorientation (40, 41) predominate in the cytolytic mechanism. Nevertheless C9's own membranolytic activity may be ascribed to its physical association with the membrane in the form of an amphiphilic polymer with the ultrastructural appearance of the classical complement lesion.

We thank Dr. Hans J. Müller-Eberhard for his continuing support and for many stimulating discussions during the progress of this work. We are grateful to Ms. Kerry Pangburn and Sarah Patthi for superb technical assistance. This research was supported by U.S. Public Health Service Grants AI 67007 and HL 16411. E.R.P. is an Established Investigator of the American Heart Association (no. 79–149). J.T. was supported by a grant from the Swiss National Science Foundation. This is publication no. 2418 from the Research Institute of Scripps Clinic.

1. Stolfi, R. L. (1968) *J. Immunol.* **100,** 46–54.
2. Hadding, U. & Müller-Eberhard, H. J. (1969) *Immunology* **16,** 719–735.
3. Rommel, F. A. & Mayer, M. M. (1973) *J. Immunol.* **110,** 637–647.
4. Frank, M. M., Rapp, H. J. & Borsos, T. (1965) in *Ciba Foundation Symposium on Complement,* eds. Wostenholme, G. E. W. & Knight, J. (Churchill, London), pp. 120–132.
5. Okada, M., Boyle, M. D. P. & Borsos, T. (1980) *Biochem. Biophys. Res. Commun.* **94,** 406–412.
6. Kolb, W. P., Haxby, J. A., Arroyave, C. M. & Müller-Eberhard, H. J. (1972) *J. Exp. Med.* **135,** 549–566.
7. Kolb, W. P. & Müller-Eberhard, H. J. (1974) *J. Immunol.* **113,** 479–488.
8. Podack, E. R., Biesecker, G., Kolb, W. P. & Müller-Eberhard, H. J. (1978) *J. Immunol.* **121,** 484–490.
9. Boyle, M. D. P. & Borsos, T. (1979) *J. Immunol.* **123,** 71–76.
10. Boyle, M. D. P., Gee, A. P. & Borsos, T. (1979) *J. Immunol.* **123,** 77–82.
11. Podack, E. R., Stoffel, W., Esser, A. F. & Müller-Eberhard, H. J. (1981) *Proc. Natl. Acad. Sci. USA* **78,** 4544–4548.
12. Hu, V. W., Esser, A. F., Podack, E. R. & Wisnieski, B. J. (1981) *J. Immunol.* **127,** 380–386.
13. Dourmashkin, R. R. (1978) *Immunology* **35,** 205–212.
14. Podack, E. R., Esser, A. F., Biesecker, G. & Müller-Eberhard, H. J. (1980) *J. Exp. Med.* **151,** 301–313.
15. Podack, E. R. & Müller-Eberhard, H. J. (1980) *J. Immunol.* **124,** 1536 (abstr.).
16. Biesecker, G., Podack, E. R., Halverson, C. A. & Müller-Eberhard, H. J. (1979) *J. Exp. Med.* **149,** 448–458.
17. Podack, E. R. & Müller-Eberhard, H. J. (1981) *J. Biol. Chem.* **256,** 3145–3148.
18. Ware, C. F., Wetsel, R. H. & Kolb, W. P. (1981) *Mol. Immunol.* **18,** 521–531.
19. Bhakdi, S. & Tranum-Jensen, J. (1979) *Proc. Natl. Acad. Sci. USA* **76,** 5872–5876.
20. Bhakdi, S. & Tranum-Jensen, J. (1981) *Proc. Natl. Acad. Sci. USA* **78,** 1818–1822.
21. Hammer, C. H., Wirtz, G. H., Renfer, L., Gresham, H. D. & Tack, B. F. (1981) *J. Biol. Chem.* **256,** 3995–4006.
22. Biesecker, G. & Müller-Eberhard, H. J. (1980) *J. Immunol.* **124,** 1291–1296.
23. Podack, E. R., Kolb, W. P., Esser, A. F. & Müller-Eberhard, H. J. (1979) *J. Immunol.* **123,** 1071–1077.
24. Kolb, W. P. & Müller-Eberhard, H. J. (1976) *J. Exp. Med.* **143,** 1131–1139.
25. Seegan, G., Smith, C. & Schumaker, V. (1979) *Proc. Natl. Acad. Sci. USA* **76,** 907–911.
26. Wetsel, R. H., Jones, M. A. & Kolb, W. P. (1980) *J. Immunol. Methods* **35,** 319–335.
27. Dalmasso, A. & Müller-Eberhard, H. J. (1966) *Immunochemistry* **3,** 497 (abstr.).
28. Monahan, J. B. & Sodetz, J. M. (1980) *J. Biol. Chem.* **255,** 10579–10582.
29. Steckel, E. W., York, R. G., Monahan, J. B. & Sodetz, J. M. (1980) *J. Biol. Chem.* **255,** 11997–12005.
30. Tschopp, J. & Podack, E. R. (1981) *Biochem. Biophys. Res. Commun.* **100,** 1409–1414.
31. Tranum-Jensen, J., Bhakdi, S., Bhakdi-Lehnen, B., Bjerrum, O. J. & Speth, V. (1978) *Scand. J. Immunol.* **7,** 45–56.
32. Mayer, M. M. (1976) in *The Nature and Significance of Complement Activation,* International Symposium (Ortho Res. Inst. Med. Sci., Raritan, NJ), pp. 29–41.
33. Giavedoni, E. B. & Dalmasso, A. P. (1979) *J. Immunol.* **122,** 240–245.
34. Michaels, D. W., Abramovitz, A. S., Hammer, C. H. & Mayer, M. M. (1976) *Proc. Natl. Acad. Sci. USA* **73,** 2852–2856.
35. Simone, C. B. & Henkart, P. (1980) *J. Immunol.* **124,** 954–963.
36. Sims, P. L. & Lauf, P. K. (1978) *Proc. Natl. Acad. Sci. USA* **75,** 5669–5673.
37. Sims, P. L. & Lauf, P. K. (1980) *J. Immunol.* **125,** 2617–2625.
38. Ramm, L. E. & Mayer, M. M. (1980) *J. Immunol.* **124,** 2281–2287.
39. Mayer, M. M. (1972) *Proc. Natl. Acad. Sci. USA* **69,** 2954–2958.
40. Podack, E. R., Biesecker, G. & Müller-Eberhard, H. J. (1979) *Proc. Natl. Acad. Sci. USA* **76,** 897–901.
41. Esser, A. F., Kolb, W. P., Podack, E. R. & Müller-Eberhard, H. J. (1979) *Proc. Natl. Acad. Sci. USA* **76,** 1410–1414.